



THE SEA OF TWO COUPLED PLATES: AN INVESTIGATION INTO THE EFFECTS OF SUBSYSTEM IRREGULARITY

B. R. MACE

*Department of Mechanical Engineering, University of Auckland, Private Bag 92019,
Auckland, New Zealand*

AND

J. ROSENBERG*

RAFAEL, Department 42, PO Box 2250, Haifa, Israel

(Received 28 August 1996, and in final form 17 October 1997)

A system comprising two edge-coupled plates is considered. Theoretical predictions of the coupling power and coupling loss factor are made using traditional, “asymptotic” SEA wave theory and an analytical wave solution application to rectangular plates. These are compared to numerical frequency averages found by FEA of the complete system. Results are presented for variously shaped plates and different levels of damping. If the damping is large enough (i.e., for “weak” coupling) the response is independent of the shape of the plates. For lighter damping (i.e., “strong” coupling) the response depends significantly on the specific geometry of each plate: the coupling power is often substantially less than that predicted by traditional SEA theory, which also overpredicts the coupling loss factor. Both the coupling power and coupling loss factor are least for rectangular plates, for which the irregularity of the subsystems is least. The reasons for this behaviour are attributed to wave coherence or, in modal terms, to localisation of the global modes of the structure within one or other subsystem. A parameter γ_0 is given which provides an estimate of the strength of coupling. This parameter arises in the analysis of coupled rectangular plates and gives a conservative estimate for irregularly shaped plates.

© 1998 Academic Press Limited

1. INTRODUCTION

The analysis of higher frequency vibrations brings special difficulties. Conventional deterministic (i.e., “exact”) methods such as finite element analysis (FEA) become inaccurate, partly because of the sheer size of the models required but primarily because of the sensitivity of the response of the system to small details in its construction, its properties and its boundary conditions, which are not known to sufficient accuracy. Therefore alternative energy-based approaches, such as statistical energy analysis (SEA) [1, 2], are often adopted. Such theories aim to predict the ensemble and/or frequency average response of a system in terms of a few, gross, physical and geometric system properties.

This paper concerns the SEA of a system which comprises two coupled plates. Comparisons are made between SEA theories and broadband frequency average responses calculated from FEA of plates of differing geometries. The intentions are to investigate the effects of varying levels of damping (whether measured by loss factor, modal overlap or base reflectance) and of subsystem irregularity on the accuracy of SEA predictions.

*Some of this work was performed while the second author was on sabbatical leave at the University of Auckland.

Another intention is to examine the strength of coupling between the plates—this is quantified in [3] for the case of rectangular plates, but the extent to which conclusions drawn from [3] are applicable to plates of arbitrary geometry is unknown.

In the next section the SEA model of the two-plate system is described, the SEA equations stated and results from two wave theories reviewed. These theories are the traditional, asymptotic wave approach [1] and an analytical theory [3] for the case of rectangular plates. Section 3 outlines the method by which a finite model of the whole system was made and FEA results cast in SEA form [4]. Numerical examples are presented and discussed in section 4.

2. SEA AND WAVE THEORIES

In SEA a system is regarded as comprising a number of subsystems coupled together. Excitations inject energy into the subsystems. The energy flows through the couplings to other parts of the system, eventually being dissipated by damping. The response of a particular subsystem is described by the time and space average energy within it. System properties are not known exactly, but are drawn from some statistically defined ensemble. Theoretical predictions are made of the average response of all systems within the ensemble. The response of an individual ensemble member system will normally differ from this ensemble average. However, it is assumed that the frequency average response of an individual system equals the ensemble average to an acceptable accuracy if the bandwidth is wide enough such that it contains many modes of vibration.

Central to such energy flow approaches is the estimation of input and coupling powers. In SEA it is normally assumed that the coupling power between two subsystems is proportional to the difference in their energy densities (or mean modal energies), the central problem now becoming the estimation of the coupling loss factor. Approaches to SEA, whether along modal or wave lines, involve a number of assumptions, and the SEA method is generally held to be accurate for “weak” rather than “strong” coupling, although there is no quantitative, widely-accepted definition of what is meant by “weak” and “strong” coupling strengths.

2.1. THE SEA EQUATIONS FOR TWO COUPLED PLATES

The system considered here is shown in Figure 1 and comprises two thin, flat, uniform plates a and b joined uniformly along a straight edge, each plate forming one subsystem. The length of the coupling is (nominally) d and the areas of the plates are A_a and A_b . It is assumed that only plate a is excited and that the excitation is time-harmonic “rain-on-the-roof” at frequency ω and of constant magnitude $F^2 \text{ N}^2/\text{m}^2$. Such excitation

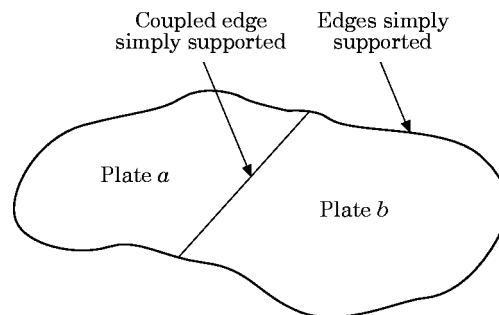


Figure 1. System comprising two, edge-coupled plates. Plate a is excited by “rain-on-the-roof”.

is equivalent to averaging the energy response to point force excitation over all possible points of application of the force. (If instead plate b is excited, results can be obtained by exchanging the subscripts a and b in what follows.) For broadband excitation, it is additionally assumed that the excitation is random, stationary and of constant power spectral density.

From conservation of energy consideration it follows that

$$P_{in} = P_{diss,a} + P_{ab}, \quad 0 = P_{diss,b} - P_{ab}, \quad (1)$$

where P_{in} , P_{diss} and P_{ab} are the input, dissipated and coupling powers (a list of symbols is given in the Appendix). All powers and energies are implicitly assumed to be time averages. In SEA applications, individual systems are assumed to be drawn at random from an ensemble of systems, although this is sometimes not explicitly stated. Uncertainty exists in that the properties of each system vary about some nominal values across the ensemble. The uncertainty may be expressed in terms of physical and geometric properties, in terms of modal properties (for example that the distribution of natural frequencies is random) or in terms of wave properties, as described in section 2.2 below. In theoretical studies, equation (1) may then be ensemble averaged. The dissipated powers are, to a good approximation, given by

$$\langle P_{diss,a} \rangle = \omega \eta_a \langle E_a \rangle, \quad \langle P_{diss,b} \rangle = \omega \eta_b \langle E_b \rangle, \quad (2)$$

where $\langle \cdot \rangle$ denotes the ensemble average, E is the subsystem total energy, η the damping loss factor and ω the frequency of excitation. The assumption of coupling power proportionality is that

$$\langle P_{ab} \rangle = \omega n_a \eta_{ab} (\langle D_a \rangle - \langle D_b \rangle), \quad (3)$$

where η_{ab} is the coupling loss factor and where $\langle D \rangle = \langle E \rangle / n$ is the energy density, or mean modal energy, n being the asymptotic modal density of the subsystem. For a plate, n is given by

$$n(\omega) = (A/4\pi) \sqrt{m/B}, \quad (4)$$

where m is the mass per unit area and B the bending stiffness [2]. The SEA equations (1–3) enable the ensemble average response to be predicted if the input power and coupling power (or coupling loss factor) are known, or alternatively may be used to define the coupling loss factor for given input and coupling powers by

$$\eta_{ab}/\eta_a = \langle P_{ab} \rangle / \langle P_{in} \rangle / [1 - (\langle P_{ab} \rangle / \langle P_{in} \rangle) (1 + M_a/M_b)], \quad (5)$$

where $M = \omega \eta n = \omega \Delta$ is the modal overlap, Δ being the half-power bandwidth.

In applications, equations (2, 3, 5) are assumed to hold to acceptable accuracy when frequency average powers \bar{P}_{in} and \bar{P}_{ab} are taken, instead of ensemble averages. However, ensemble and frequency averages are not the same, and terms such as “SEA-like” and “apparent” coupling loss factor have been used to distinguish the frequency average behaviour of an individual system from that of the ensemble (e.g., [5]).

The system comprising two coupled plates is a common application in the SEA literature. Systems comprising two rectangular plates have been considered in many papers. In [6, 7], the responses of individual systems were predicted numerically using global modes of vibration. In [8] the system properties were randomly varied to obtain numerical responses which were then averaged over an ensemble of systems, while in [3] a wave analysis was performed, and the deterministic results then ensemble averaged. Finite element methods have also seen application, both in determining subsystem properties such as modal density and in forming global system models for comparison with SEA theories [5, 9].

2.2. ASYMPTOTIC SEA WAVE THEORY

In the classical wave approach for the estimation of coupling power and coupling loss factor [1] a number of assumptions and approximations are made. First, the subsystems are assumed to be reverberant, in that the amplitude of a wave decays by a small amount as it propagates across the subsystem. Secondly, it is assumed that diffuse wave fields are incident upon the coupling. The third assumption is that the two wave trains incident upon the coupling are incoherent, so that the transmission due to each alone can be superposed. This would be the case if the receiving subsystem extended to infinity. If the transmission coefficient (defined in terms of power wave amplitudes) of the coupling is T , then the proportion of the incident energy that is transmitted to the receiving subsystem is given by \bar{T}^2 , the average of T^2 over all incident angles. Thus the coupling power is

$$P_{ab} = \bar{T}^2 P_{inc,a} - \bar{T}^2 P_{inc,b}, \quad (6)$$

where P_{inc} is the power in the incident wave. Fourthly, the assumption is made that the coupling is “weak” in the sense that $T^2 \ll 1$, so that the wave reflected back into the excited subsystem is of virtually the same amplitude as the incident wave. Since the subsystems are reverberant, their energies can be estimated from the amplitudes of the waves incident on the coupling so that

$$P_{inc,a} = E_a c_{g,a} d / \pi A_a, \quad (7)$$

where c_g is the group velocity in the plate. The coupling loss factor is thus

$$\eta_{\infty} = 2\bar{T}^2 d / \pi k_a A_a, \quad (8)$$

$k = \sqrt[4]{m/B} \sqrt{\omega}$ being the wavenumber.

In this classical theory the shape of the plates is irrelevant. Experience shows that the above estimate is most accurate for systems where the modal overlap is high, and for this reason this theory will be referred to here as an “asymptotic” theory. It is also found that accuracy is best for subsystems with high dimensionality and whose geometries are highly irregular.

Sometimes the asymptotic theory fails to predict accurately the broad band frequency average response. The reasons for this failure can be traced primarily to the third assumption, that regarding the coherence of waves incident on the coupling, since equations (6) and (8) can be poor estimates even if all the other assumptions are satisfied. If the subsystems are finite, the waves reflected from the coupling will eventually be reflected from the subsystems to return to the coupling. The third assumption is therefore equivalent to assuming that the ensemble and/or frequency average effects of this coherent reflected wave are negligible, and this is not necessarily the case [10].

2.2. ANALYTICAL WAVE THEORY FOR RECTANGULAR PLATES

The wave analysis of [3] concerns specifically the case of two rectangular plates whose edges are simply supported. The response is expressed in terms of wave components, each component having a unique trace wavenumber along the coupling. Since the plates and coupling are uniform, the components propagate independently through the system and the total response is given by the sum of the responses due to each trace wavenumber component. Expressions for the input and coupling powers for individual systems are found. The analysis requires none of the assumptions made in the asymptotic theory and in particular the effects of reflections within the subsystems and wave coherence are taken fully into account. The contribution of near fields to the response and energy flows is, however, neglected.

The independent trace wavenumber components behave dynamically like the one-dimensional systems discussed in [11]. There, the ensemble is defined by including uncertainty in the phase changes experienced by waves travelling once around each subsystem. Since the coupling and input powers depend on these phases mod 2π , the phases are assumed to be random and (mod 2π) uniformly probable in $[0, 2\pi]$. This is equivalent to assuming that no specific phases are preferred: it is reasonable in that the absolute phase changes are very large, so that they are sensitive to small levels of uncertainty in system properties and also that, when frequency averaged, the phases change rapidly with frequency so that frequency and ensemble averages become equal, at least in many situations [12]. It is also broadly equivalent to the assumption often made in modal approaches, that the uncoupled subsystem modal behaviour is such that there is a uniform probability that a subsystem natural frequency occurs at any specific frequency. In [11] it was found that, for one-dimensional systems, the strength of coupling can be described in terms of two parameters, γ and δ , which depend on the transmission coefficient of the coupling and the levels of damping within the two subsystems. For weak coupling $\gamma < 1$, energy essentially “leaks” through the coupling and the traditional wave estimates of the coupling power and coupling loss factor are accurate. For strong coupling $\gamma > 1$ there is in effect a sharing of energy between the two subsystems. In this case the asymptotic wave theory gives poor estimates of coupling power and coupling loss factor. (The parameter δ is only important in extreme cases where both subsystems are reverberant and one is very lightly damped compared to the other—such cases will not be considered further here.)

The assumptions concerning the ensemble of plate systems in [3] are similar, in that it is assumed that the phase changes experienced by waves travelling back and forth across the width of the plates or across the length of either plate are random and uniformly probable in $[0, 2\pi]$. If the plates have the same wavenumbers, then the ensemble averages of the input and coupling powers are given by [3]

$$\begin{aligned} \langle P_{in} \rangle &= P_{in,\infty} (1 - 1/k_a d), & P_{in,\infty} &= F^2 A_a / 16 \sqrt{Bm} \\ \langle P_{ab} \rangle &= P_{in,\infty} \frac{1}{\pi \mu_{a0}} \left\{ \int_0^1 \frac{T^2(\kappa)}{\sqrt{(1 + \gamma^2(\kappa))(1 + \delta^2(\kappa))}} d\kappa - \frac{\pi T^2(0)}{2k_a d \sqrt{(1 + \gamma^2(0))(1 + \delta^2(0))}} \right\}, \end{aligned} \quad (9)$$

where κ is the ratio of the trace wavenumber to the wavenumber in the excited plate, $P_{in,\infty}$ is the power input to a uniform, infinite plate due to an excitation of magnitude ($F^2 A_a$) where

$$\begin{aligned} \gamma^2 &= T^2 \cosh^2 \mu_d / \sinh \mu_a \sinh \mu_b, & \delta^2 &= T^2 \sinh^2 \mu_d / \sinh \mu_a \sinh \mu_b, \\ \mu(\kappa) &= \mu_0 / \sqrt{1 - \kappa^2}, & \mu_0 &= kln/2 = \pi \eta l / \lambda, & \mu_d &= (\mu_a - \mu_b) / 2. \end{aligned} \quad (10)$$

Here $l = A/d$ is the length of the rectangular plate and λ the bending wavelength. The attenuation parameters μ_a and μ_b , termed the subsystem reflectances in [3, 11], represent the effects of damping in the subsystems, They are such that the amplitude of a wave with trace wave number κk , which propagates from the coupling to the end of the plate and back to the coupling, reduces by the factor $\exp(-\mu)$. The base reflectances $\mu_{a0} = \mu_a(0)$ and μ_{b0} play a special role in determining the responses. Since μ is an increasing function of κ , they represent the minimum attenuation experienced by any wave component.

For the two-plate system, the coupling parameters $\gamma(\kappa)$ and $\delta(\kappa)$ are functions of the trace wavenumber, as is the transmission coefficient $T(\kappa)$. Generally, some of the trace

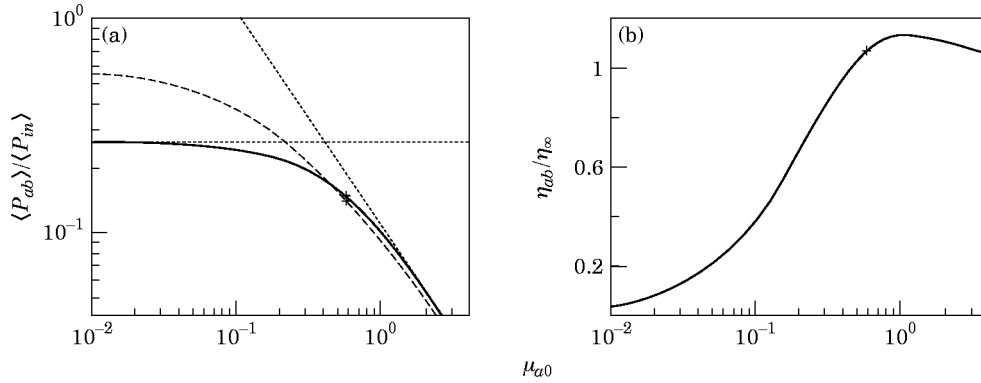


Figure 2. Theoretical SEA predictions: (a) coupling power; —, theory, rectangular plates [3]; ----, asymptotic wave theory; ·····, low and high μ_0 limits. (b) coupling loss factor; —, rectangular plates [3]. $\gamma_0 = 1$.

wavenumber components are strongly coupled and some are weakly coupled. The total energy flows between the plates are however normally dominated by the strongly coupled components. For the case where the coupling is a simple support

$$T^2 = (1 - \kappa^2)/2, \quad \bar{T}^2 = 1/3. \quad (11)$$

Now γ is a decreasing function of κ , so that the maximum value is $\gamma_0 = \gamma(0)$. If $\gamma_0 < 1$, then all the wave components are weakly coupled. If $\gamma_0 > 1$, some wave components are strongly coupled and some weakly coupled.

2.3. NUMERICAL EXAMPLE

Figure 2 shows the ensemble average coupling power and the coupling loss factor for the case where the line of coupling is simply supported, the plates have nominally the same thickness, are made from the same material, are wide and the length ratio $l_b/l_a = 1.4$. The value of μ_{a0} for which $\gamma_0 = 1$ is indicated, this representing the transition from strong to weak coupling. The estimate of coupling power given by the asymptotic theory is also shown, and can clearly be significantly in error in the strong coupling regime, where it substantially over-predicts both the coupling power and the coupling loss factor.

For rectangular plates the strength of coupling, and hence the physical features of the response, depend on the coupling parameter γ_0 . This in turn depends on the attenuation parameter μ_0 (i.e., the base reflectance) and not the modal overlap M , as is sometimes maintained. (The two parameters are however related, since $M = \mu_0 kd/2\pi = \omega\eta n$, but they are not equivalent since the wavenumber and width of the coupled edge is also involved.) This dependence on μ_0 is perhaps not surprising, if one considers the consequence of increasing the width of the plates. Now the modal overlap increases, since the modal density is proportional to plate area, but the input and coupling powers per unit length of coupling, their ratio and the plate energy densities all remain constant.

3. FINITE ELEMENTS AND SEA

The method used to obtain finite element results and then cast them in SEA form is the global approach described in [4]. The aim in this paper is to determine the response of the system to time harmonic “rain-on-the-roof” excitation, the response quantities of interest being the system and subsystem time average potential and kinetic energies and the time average input, coupling and dissipated powers. This time harmonic response is then

frequency averaged as required. The response to “rain” excitation is regarded as being equivalent to averaging the responses to individual point excitations applied at all possible excitation points.

The steps involved are briefly as follows. First the system is discretized and mass and stiffness matrices determined. In the examples below this was done using a commercial finite element package, ANSYS. Such packages, however, are not well suited to determining the response to time-harmonic “rain”, so subsequent processing was performed using Matlab. Expressions for system response quantities (energies, powers, etc.) are developed. The next step is to determine the response to a time harmonic point force. This decomposed into global modes of vibration (i.e., modes of the whole system) to make further calculations more time-efficient. Finally the response to time harmonic point “rain-on-the-roof” excitation is found.

4. NUMERICAL INVESTIGATION

Numerical investigations were performed on a number of different 2-plate systems as described below. Finite element predictions under various damping conditions were frequency averaged and compared with the SEA theories described above.

4.1. SYSTEM DESCRIPTION

4.1.1. *Physical and geometric properties*

Each system comprised two, straight-edged plates which were edge-coupled. All edges, including the line of coupling, were simply supported. In all cases the plates were of the same material (steel), with the properties given in Table 1. In all cases the length of the coupled edge was 0.9 m and the areas of the smaller and larger plates were 0.9 m² and 1.26 m². Systems comprising plates of differing shapes were analysed, the shapes being either rectangular (R), distorted rectangular pentagon (D) (with the two sides adjacent to the coupling perpendicular to the coupled edge) or pentagonal (P) as shown in Figure 3. The plate areas were chosen so that the length ratio of the rectangular plates was 1.4, this number being such as to reduce possible “modal line-up” effects when frequency averages were subsequently taken [12]. One plate was assumed to be excited by “rain” of unit amplitude.

The shapes offer different amounts of irregularity, and all 9 possible combinations of two plates were analyzed (e.g., RR, RP, PR etc.). In each case in the post-processing either the smaller or larger plate could be excited, giving 18 different FE/SEA analyses.

The transmission coefficient of the coupling is given in equation (11). The modal densities are independent of frequency and are given in Table 1.

4.1.2. *FEA*

FEA was performed using ANSYS. A total of 408 shell elements (type 63) were used, giving a total of 1155 nodal degrees of freedom. Of these, 363 were retained as “master”

TABLE 1
Physical and geometric properties (SI units)

Elastic modulus	2×10^{11}	Length of coupled edge	0.9
Density	8×10^3	Plate area (a, b)	0.9, 1.26
Poisson's ratio	0.3	Modal density (a, b)	0.0297, 0.0416
Thickness	0.01	System total modal density	0.0714

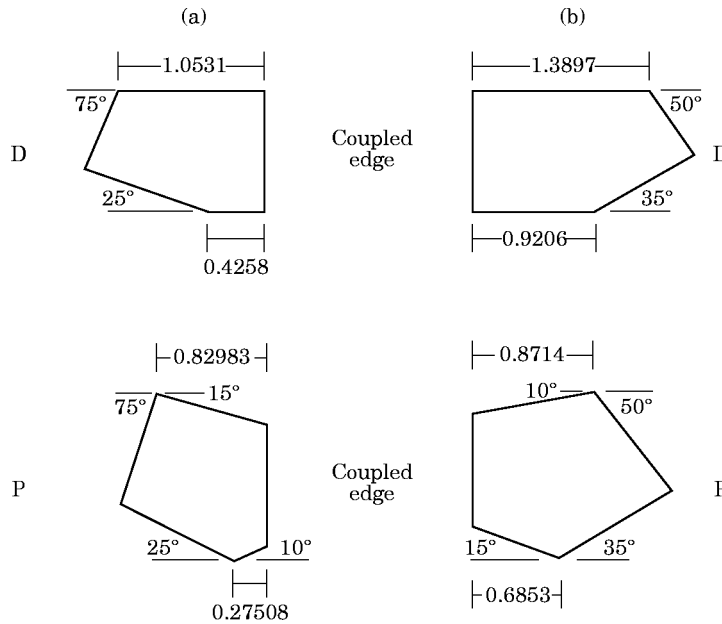


Figure 3. Plate shapes: (a) smaller plate and (b) larger plate.

degrees of freedom, these being the out-of-plane displacements. Mass and stiffness matrices, natural frequencies and mode shapes were found. The model gave acceptable accuracy for frequencies up to 2 kHz and above.

4.1.3. Post-processing: damping and frequency averaging

The amount of damping in the system can be described variously by the damping loss factor η , the bandwidth $\Delta = \omega\eta$, the modal overlap $M = n\Delta$ (specified either for plate a or plate b or in terms of the global modes of the whole system) or the base reflectance μ_0 , which for the rectangular plates here is given by $\mu_0 = \eta kl/2$, at least for small η . For non-rectangular plates the effective base reflectance is assumed to be $\mu_0 = \eta kA/2d$. For rectangular plates the base reflectance is the appropriate parameter to describe the effects of damping.

When post-processing the finite element results to determine the discrete frequency response, the loss factor can be assumed to be dependent on frequency. This can be done so as to maintain the same "amount" of damping over the whole frequency range (i.e., to make the base reflectance or the modal overlap independent of frequency). Two different damping models were considered, although results will be given primarily for the first. In this, the loss factor is assumed to vary as $\omega^{-1/2}$, so that μ_0 is frequency independent. In the second damping model, the loss factor varies with frequency as ω^{-1} , in which case the modal overlap (and the half-power bandwidth) is constant. In both cases the loss factor is assumed to be the same for both plates. Values used for the damping parameters are given in Table 2.

Frequency averaging was performed by averaging discrete frequency responses calculated at frequencies whose resolution was less or equal to one-quarter of the half-power bandwidth. Numerical integration was used here rather than the approximate, closed form integrals given in [4]. Response components were calculated for all modes retained in the finite element analysis and not just those modes resonant in the frequency band.

TABLE 2

Damping parameters. Corresponding entries in each column yield the same amount of damping at 1 kHz

η	0.004	0.007	0.01	0.02	0.04	0.07	0.1	0.2
μ_{a0}	0.0408	0.0713	0.102	0.204	0.408	0.713	1.019	2.038
$M = M_a + M_b$	0.286	0.500	0.714	1.43	2.86	5.00	7.14	14.3
Δ (Hz)	4	7	10	20	40	70	100	200

4.2. DISCRETE FREQUENCY RESPONSE

As an example of discrete frequency response, Figure 4 shows the input and coupling powers for RR and PP plates at a constant total modal overlap (i.e., modal overlap based on the total, global modal density). The half-power bandwidth is 7 Hz, the loss factor 0.007 at 1 kHz. Clear resonant behaviour can be seen. There are also qualitative differences between the powers for RR and PP plate systems, the variation for RR plates being greater, particularly with regard to the coupling power.

4.3. FREQUENCY AVERAGE RESPONSE

Frequency averages were calculated by averaging over a 400 Hz bandwidth. This contains on average about 12 and 16 “uncoupled” natural frequencies of the individual plates, about 28 global natural frequencies. Thus the effects of there being a finite number of modes within this band would be expected to be small.

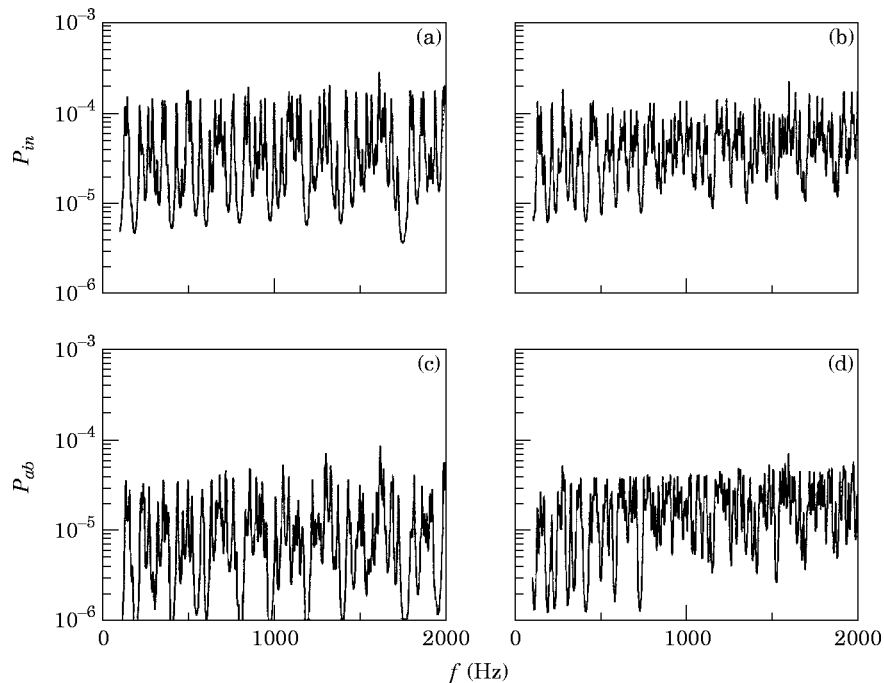


Figure 4. Discrete frequency response, constant modal overlap $M = 0.5$: (a) input power, RR plates; (b) input power, PP plates; (c) coupling power, RR plates; (d) coupling power, PP plates.

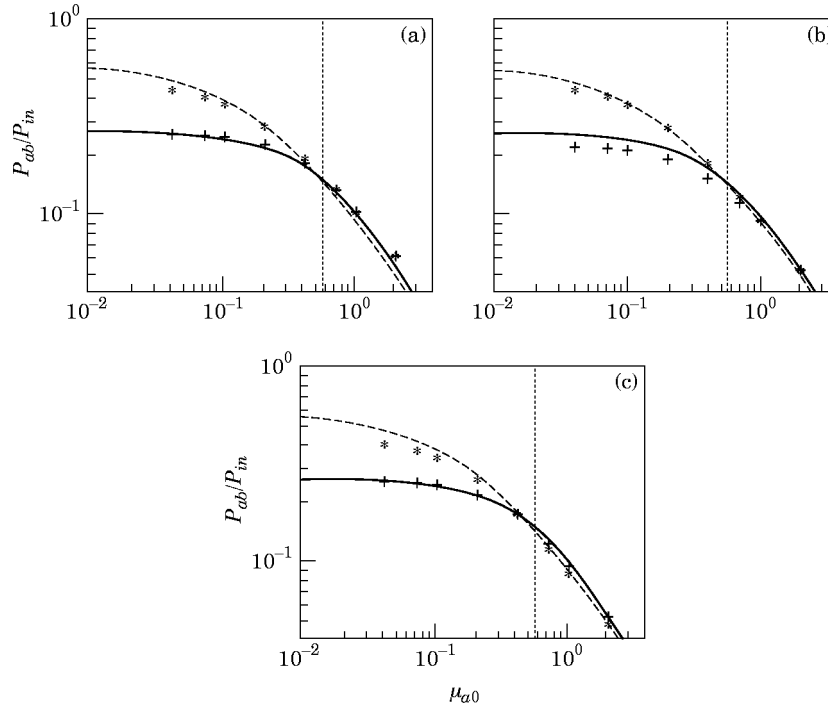


Figure 5. Coupling power as a function of base reflectance of driven plate, smaller plate excited: centre frequency at (a) 500 Hz; (b) 1000 Hz; (c) 1500 Hz. Ensemble averages: —, theory, rectangular plates; ----, asymptotic wave theory. FE frequency averages: +RR plates; *PP plates. $\cdots\cdots\cdots$, $\gamma_0 = 1$.

4.3.1. Input power

The frequency average input powers \bar{P}_in are approximately equal to the asymptotic, ensemble average expression of equation (9) [2]. Apart from minor fluctuations, varying levels of damping do not influence the average input power. Differences can be attributed to finite-width and finite-length effects (these tending to reduce the power input by forces applied close to a boundary), to the fact that theoretical predictions ignore near-field effects and to finite element modelling errors.

4.3.2. Coupling power

Generally the variation with frequency of the frequency average coupling power \bar{P}_ab , per unit frequency average input power \bar{P}_in , is small if μ_0 is constant. There are, however, significant and substantial variations of coupling power with base reflectance (i.e., with the level of damping), and these variations themselves depend on the specific shapes of the subsystems, i.e., the amount of irregularity in the system. Examples are shown in Figures 5 and 6. These show the coupling power as a function of the base reflectance μ_0 of the driven plate at each of the 3 centre frequencies with μ_0 being independent of frequency. In Figure 5 the smaller plate is excited, while in Figure 6 the larger plate is excited. Numerical results are given for RR and PP plate systems. Also shown are the analytical expression for rectangular plates (section 2.3, equation (9)) and the estimate of coupling power provided by the asymptotic SEA wave theory described in section 2.2. The levels of reflectance where $\gamma_0 = 1$ and which, for RR plates, mark transition from strong coupling (small μ_0) to weak coupling (large μ_0), are also indicated.

Generally, for large μ_0 (weak coupling, $\gamma_0 < 1$) the FE calculated coupling powers for the actual systems and the ensemble average SEA predictions are nearly equal, differences being attributable to the causes described in the previous subsection. (Theoretical predictions also assume η is small, and this introduces some errors at higher damping levels.) For small μ_0 (strong coupling, $\gamma_0 > 1$), however, there are substantial differences between the numerical results for plates of different shape. The RR results agree well with the analytical predictions, given the fluctuations observed in the average powers as a function of frequency. The PP results agree more closely with the asymptotic SEA prediction.

This behaviour is illustrated again in Figures 7 and 8, in which numerical results for nine different 2-plate systems are shown, the smaller plate being excited. Figure 7 shows the coupling power for the nine systems at each of the 3 centre frequencies, while Figure 8 shows the coupling powers at the 3 centre frequencies for each of the 9 systems. In both figures μ_0 is constant. (In Figure 7, η and M abscissae are given at each centre frequency.) In the strong coupling region the coupling power for RR plates is the smallest, while that for PP plates (which, in a sense, have the most irregularity) is usually, but not always, the largest.

The general behaviour is clear: for large μ_0 there is little dependence on plate geometry and SEA theories give accurate predictions, while for low μ_0 the coupling power depends significantly on the specific subsystem geometry, in other words on the degree of irregularity of the subsystems. The transition between these regions can be defined by the parameter γ_0 . The reasons behind these effects of subsystem irregularity can be explained in wave or modal terms.

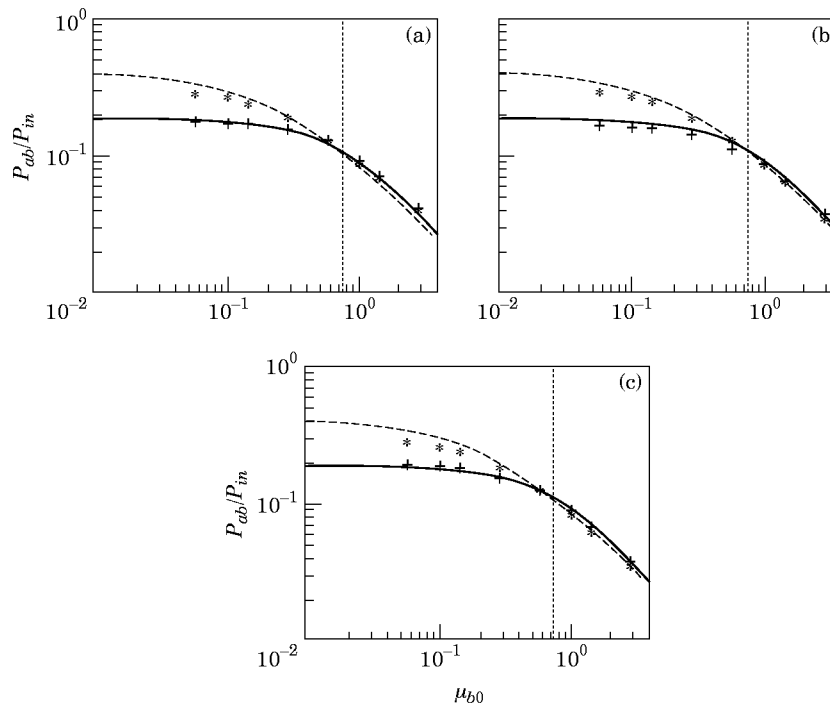


Figure 6. Coupling power as a function of base reflectance of driven plate, larger plate excited: centre frequency at (a) 500 Hz; (b) 1000 Hz; (c) 1500 Hz. Ensemble averages: —, theory, rectangular plates; ----, asymptotic wave theory. FE frequency averages: +RR, *PP plates. $\cdots\cdots\cdots$, $\gamma_0 = 1$.

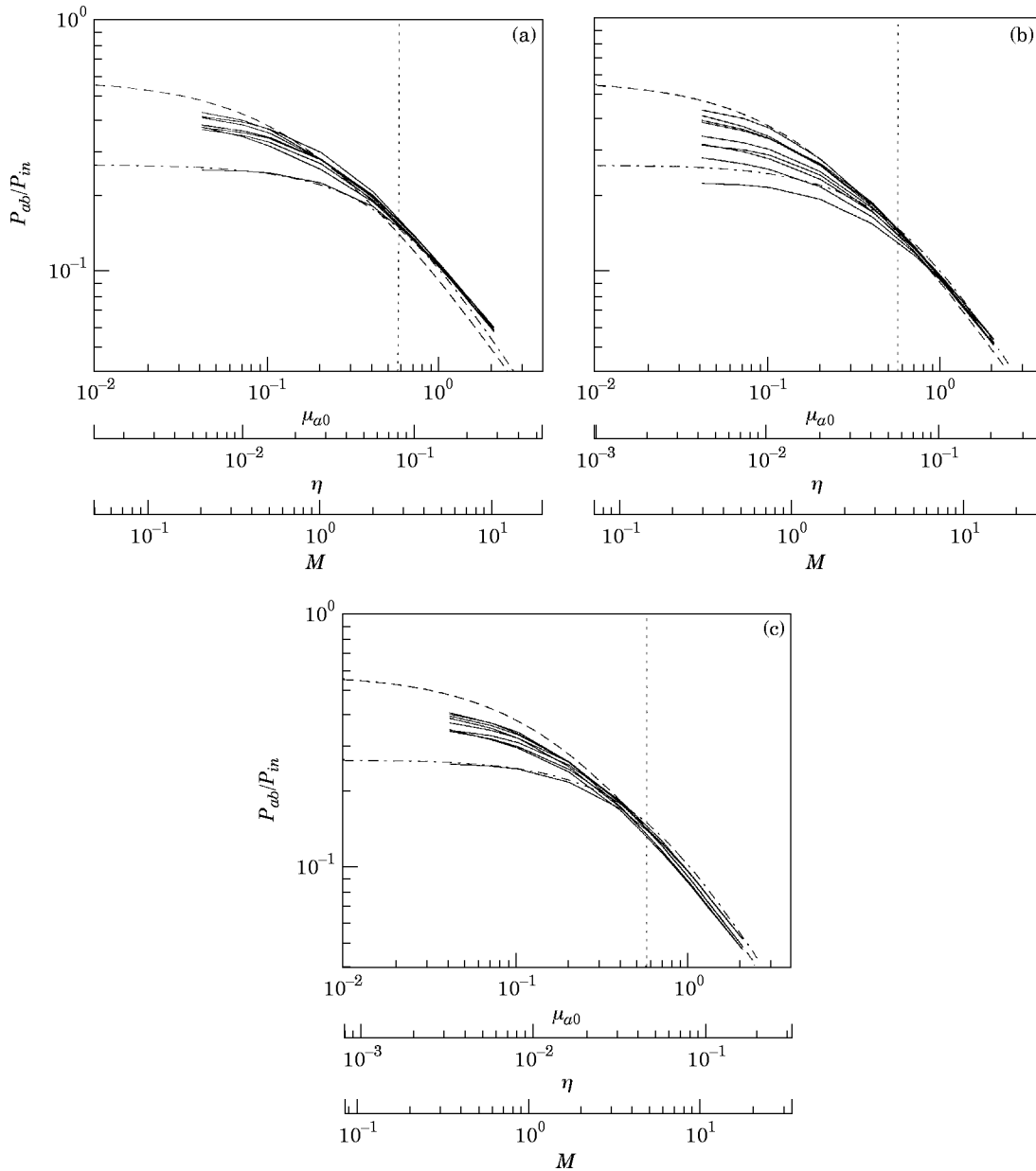


Figure 7. Coupling power as a function of base reflectance, smaller plate excited: centre frequency at (a) 500 Hz; (b) 1000 Hz; (c) 1500 Hz. Ensemble averages; -----, theory, rectangular plates; ----, asymptotic wave theory. —, FE frequency averages, 9 two-plate systems. ·····, $\gamma_0 = 1$.

4.3.2.1. Subsystem irregularity and wave coherence. From a wave perspective, subsystem irregularity affects the degree to which waves incident upon opposite sides of the coupling are correlated [10]. For small levels of damping, strong reflected waves are incident upon the coupling which, when ensemble or frequency averaged, give substantial coherent contributions to the net coupling power. The primary effect is to re-radiate power back from the receiving subsystem, hence reducing the coupling power from the value predicted by the asymptotic SEA wave theory. For

larger damping levels the amplitudes of the reflections are reduced and so, too, is the effect of wave coherence on the net coupling power.

When the subsystems are irregularly shaped a wave with a given trace wavenumber along the coupling will be scattered from the subsystem into wave components which arrive back at the coupling with different trace wavenumbers: the wave field thus tends to become more diffuse. The net coherent power is reduced because wave components with different trace wavenumbers are incoherent when their interaction is averaged along the line of coupling—only the scattered component with the same trace wavenumber contributes to the coherent power, and irregularity reduces the amplitude of this component because energy is scattered into components with different trace wavenumbers. For a rectangular plate the irregularity is least, a wave is reflected back from the subsystem without change in trace wavenumber, coherence effects are strongest and the coupling power hence least.

4.3.2.2. Subsystem irregularity and global mode localisation. The effects of irregularity can also be interpreted in terms of the manner in which global mode shapes are localised within one or other subsystem [15] and some relevant results from [15] are now summarised. The response at point x_2 per unit excitation at point x_1 is given by a sum of global mode components as

$$u(\omega, x_1, x_2) = \sum_j \alpha_j(\omega) \phi_j(x_1) \phi_j(x_2), \quad \alpha_j(\omega) = 1/(\omega_j^2(1 + i\eta) - \omega^2), \quad (12)$$

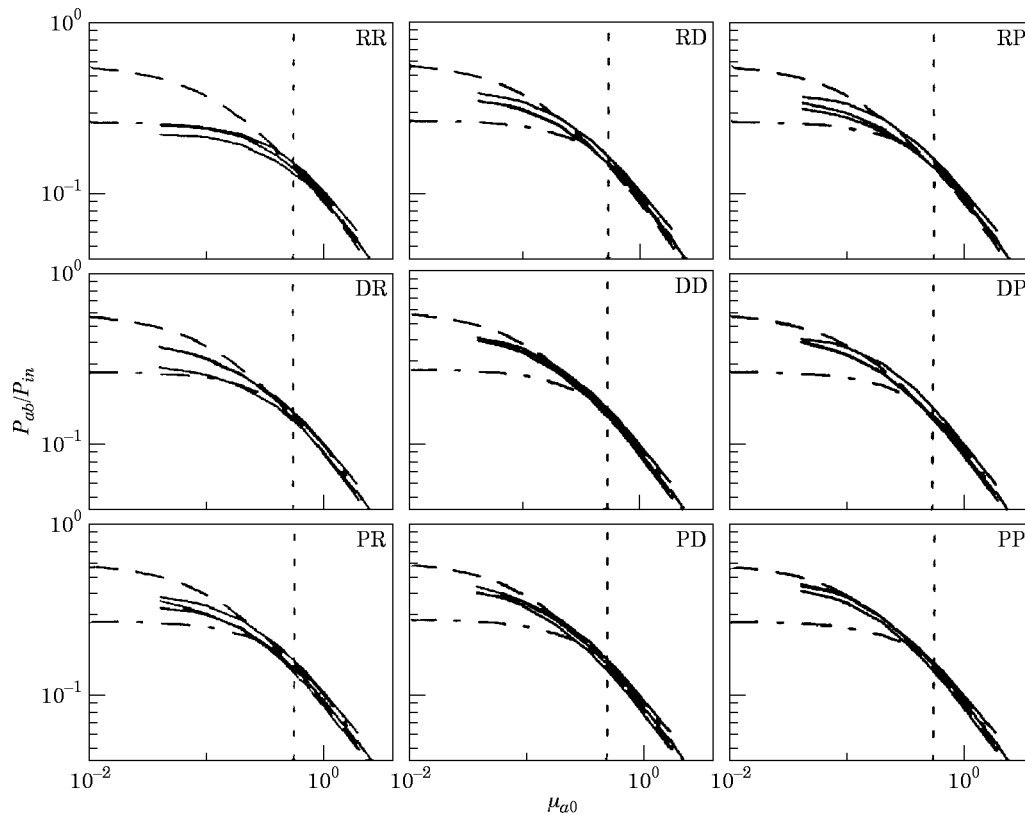


Figure 8. Coupling power as a function of base reflectance, smaller plate excited, various two-plate systems: ensemble averages: - - - -, theory, rectangular plates; ----, asymptotic wave theory, —, FE frequency averages, centre frequencies at 500 Hz, 1000 Hz and 1500 Hz. ·····, $\gamma_0 = 1$.

where $\alpha_j(\omega)$ is the modal receptance, ω_j the natural frequency and $\phi_j(x)$ the mode shape of the j th mode, mass-normalised such that

$$\int m\phi_j(x)\phi_k(x) dx = \delta_{jk}. \quad (13)$$

The time average kinetic energy density, for example, is determined by the squared response, and is given by

$$D_T = \frac{1}{4}m\omega^2|u(\omega, x_1, x_2)|^2 = \sum_{j,k} \beta_{jk}(\omega)[m\phi_j(x_1)\phi_k(x_1)][m\phi_j(x_2)\phi_k(x_2)],$$

$$\beta_{jk} = \omega^2 \operatorname{Re}\{\alpha_j\alpha_k^*\}/(4m). \quad (14)$$

The frequency average kinetic energy density taken over a bandwidth Ω is thus given by

$$\bar{D}_T = \sum_{j,k} \Gamma_{jk}[m\phi_j(x_1)\phi_k(x_1)][m\phi_j(x_2)\phi_k(x_2)], \quad \Gamma_{jk} = \frac{1}{\Omega} \int_{\Omega} \beta_{jk}(\omega) d\omega \quad (15)$$

Suppose now that excitations are applied at all points x_1 in subsystem a . The total kinetic energy in subsystem b is then found by integrating equation (15) over x_1 and x_2 and, assuming m is constant, is given by

$$\bar{T}_b = \sum_{j,k} \Gamma_{jk}\psi_{jk}^{(a)}\psi_{jk}^{(b)}, \quad \psi_{jk}^{(a)} = \int_{A_a} m\phi_j(x_1)\phi_k(x_1) dx_1, \quad \psi_{jk}^{(b)} = \int_{A_b} m\phi_j(x_2)\phi_k(x_2) dx_2, \quad (16)$$

where $\psi_{jk}^{(a,b)}$ is the kinetic energy distribution factor for the (j, k) th mode pair. Since the mode shapes are mass normalised,

$$\psi_{jj}^{(a)} + \psi_{jj}^{(b)} = 1, \quad \psi_{jk}^{(a)} + \psi_{jk}^{(b)} = 0, \quad j \neq k. \quad (17)$$

For $j = k$, $\psi_{jj}^{(a)}$ indicates the proportion of kinetic energy stored in subsystem a when the system vibrates in the j th mode. For $j = k$, $\psi_{jk}^{(a)}$ gives a measure of the orthogonality of the (j, k) th mode pair over subsystem a . Similar expressions can be developed for the input power and potential energy (which, when frequency averaged, is very nearly equal to the kinetic energy) [15].

Now suppose that the damping is light so that α_j shows a distinct resonance peak around its natural frequency ω_j . Then Γ_{jk} tends to be small except for those mode pairs j and k which ‘‘overlap’’, i.e., whose natural frequencies lie within each others half-power bandwidths. The terms Γ_{jj} are necessarily large. The response is therefore dominated by resonant modes. (Note however that it is the cross-modal coupling which gives rise to the coupling energy flow.)

Consider first the case where the modal overlap is small ($M \ll 1$). Now the response (i.e., the kinetic energy) in the undriven subsystem, is dominated by the terms Γ_{jj} and is given by

$$\bar{T}_b = \sum_j \Gamma_{jj}\psi_{jj}^{(a)}\psi_{jj}^{(b)}. \quad (18)$$

A large response, and hence a large coupling power, arises from those modes for which the product $\lambda_j = \psi_{jj}^{(a)}\psi_{jj}^{(b)} = \psi_{jj}^{(a)}(1 - \psi_{jj}^{(a)})$ is large. Such modes are not only relatively well

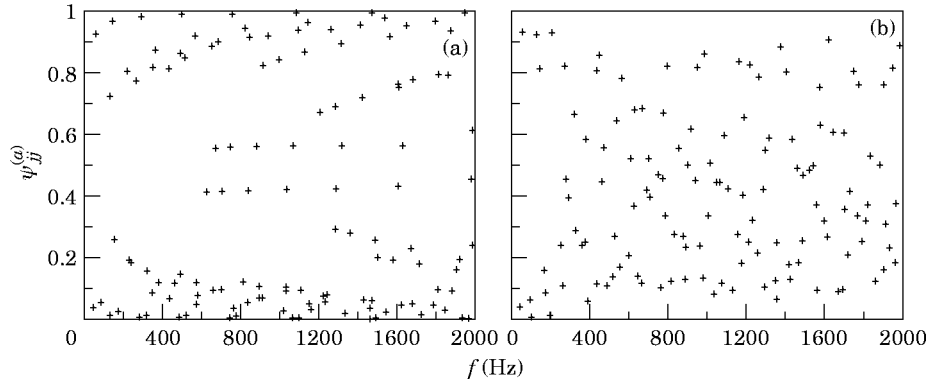


Figure 9. Kinetic energy distribution factor $\psi_{jj}^{(a)}$ for mode j as a function of frequency: (a) RR plates; (b) PP plates.

excited (i.e., $\psi_{jj}^{(a)}$ large), but also respond relatively strongly in the undriven subsystem (i.e., $\psi_{jj}^{(b)}$ large). Modes whose mode shapes are large only within one subsystem, i.e., modes which are localised within one subsystem, are either weakly excited or respond weakly, and hence give a small contribution to the response in the undriven subsystem.

Figure 9 shows the proportion $\psi_{jj}^{(a)}$ of kinetic energy stored in the smaller plate in each mode of vibration. Results for both RR and PP plates are given. There is a marked tendency for the RR global modes to be more localised, in that the energy is stored primarily within one or the other plate (i.e., $\psi_{jj}^{(a)}$ is either small or large). On the other hand, the kinetic energy for each of the global modes of the PP plates tends to be more spread out between the two plates. Figure 10 shows the cumulative probability distribution for $\psi_{jj}^{(a)}$ for the first 120 modes of each system. This illustrates again the tendency for global mode localisation to occur to a greater degree in the RR plates. Hence the response in the undriven plate and the coupling power are substantially less for the RR plates in the low μ_0 , low M region.

If the modal overlap is higher then Γ_{jk} will also be substantial for overlapping modes, typically for these modes for which $|k - j| < M$. These cross-modal terms are negative since, from the orthogonality conditions, $\psi_{kj}^{(a)}\psi_{jk}^{(b)} = -\psi_{jk}^{(a)2}$. For the PP plates they are

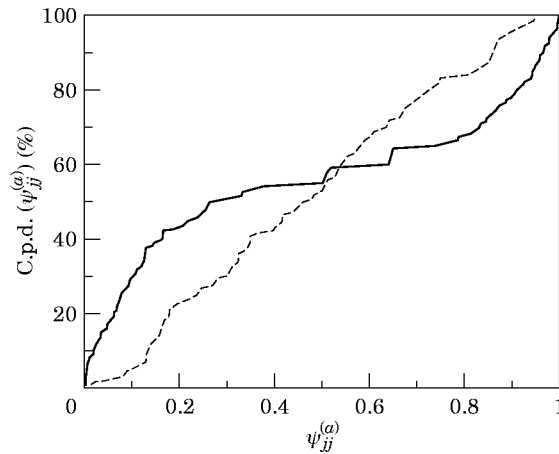


Figure 10. Cumulative probability distribution of $\psi_{jj}^{(a)}$ for the lowest 120 modes: —, RR plates; ----, PP plates.

somewhat larger in magnitude than for the RR plates and hence act to reduce the difference between their responses as modal overlap increases.

4.4. COUPLING LOSS FACTOR AND APPARENT COUPLING LOSS FACTOR

The coupling loss factor is defined in terms of ensemble average powers by equation (5), with the wave estimates being given by equations (8) and (9). Apparent coupling loss factors for specific systems and within specific frequency bands are given by equation (5) when frequency average powers are used. Examples for the plate systems discussed here are shown in Figures 11–13.

In general, for large μ_0 (i.e., large damping and weak coupling in the sense $\gamma_0 < 1$) the apparent coupling loss factor is relatively insensitive to subsystem geometry and is approximately equal to the asymptotic estimate η_∞ , although agreement is poorer at lower frequencies. For lighter damping (smaller μ_0 and strong coupling) the apparent coupling loss factor decreases and is sensitive to plate geometry. The shapes of these curves are very similar to those found in [8, 14] for plate systems with irregularity.

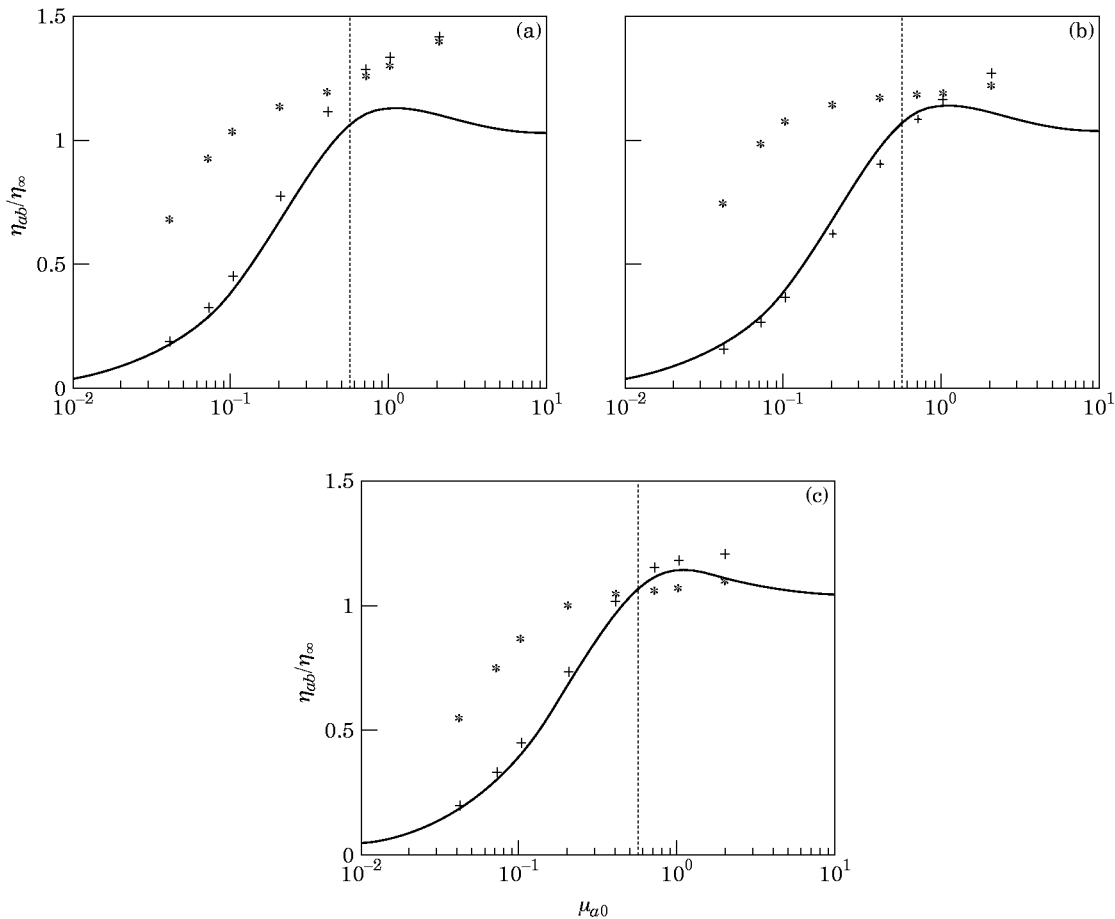


Figure 11. Coupling loss factor as a function of base reflectance, smaller plate excited: centre frequency at (a) 500 Hz; (b) 1000 Hz; (c) 1500 Hz. — theory, rectangular plates; FE frequency averages: + RR plates; * PP plates. $\cdots\cdots\cdots$, $\gamma_0 = 1$.

4.5. "RECIPROCITY"

If the SEA equations are to hold for a given system then the coupling loss factors must satisfy the relation $n_a \eta_{ab}^{(a)} = n_b \eta_{ba}^{(b)}$ [1], where the superscripts indicate which subsystem is being excited. This is often referred to as a "reciprocity" relation. It is equivalent to

$$(M_a P_{ab}^{(a)} / P_m^{(a)}) / (M_b P_{ba}^{(b)} / P_m^{(b)}) = 1, \quad (19)$$

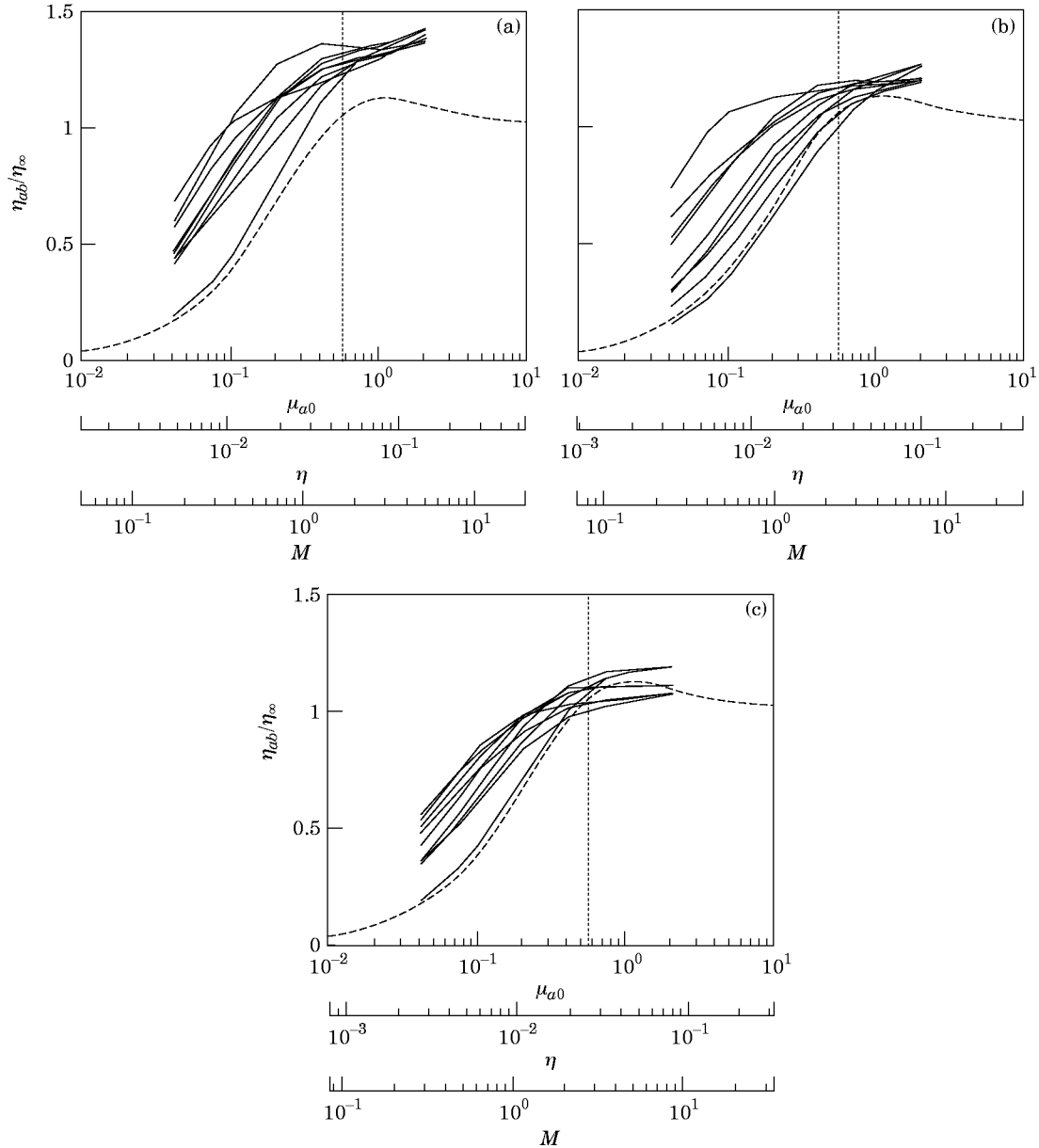


Figure 12. Coupling loss factor as a function of base reflectance, smaller plate excited: centre frequency at (a) 500 Hz; (b) 1000 Hz; (c) 1500 Hz. ----, theory, rectangular plates; —, FE frequency averages: 9 two-plate systems. ·····, $\gamma_0 = 1$.

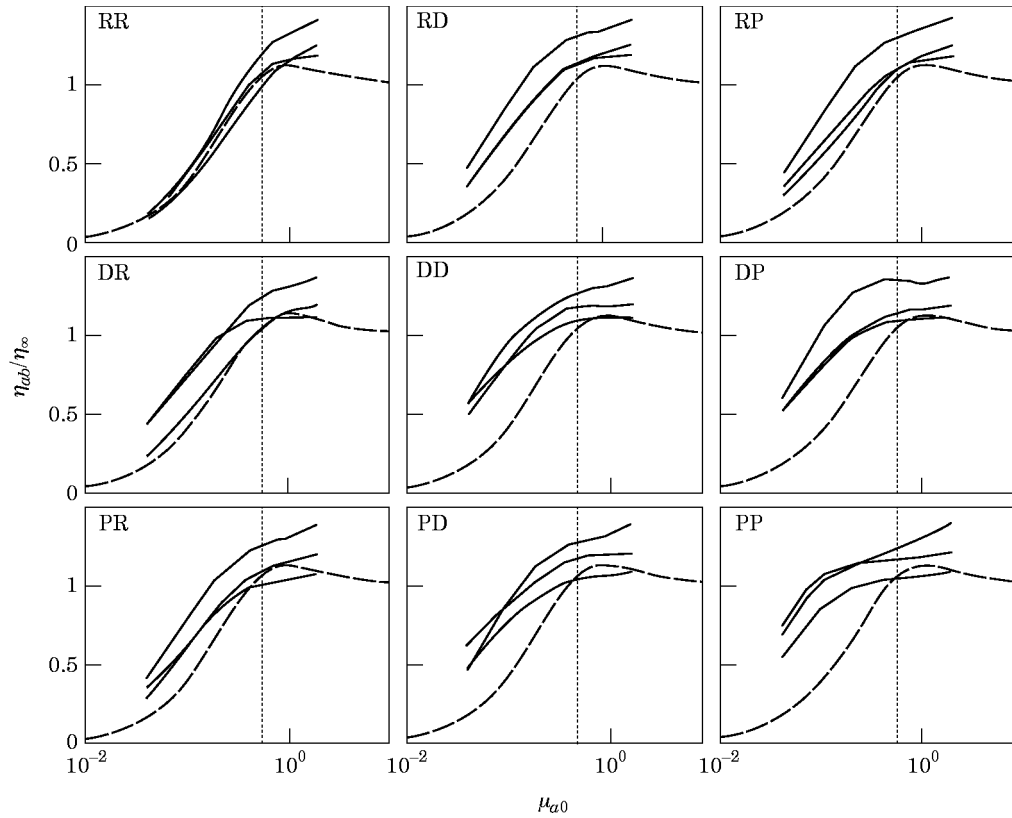


Figure 13. Coupling loss factor as a function of base reflectance, smaller plate excited, various two-plate systems. ----, theory, rectangular plates; —, FE frequency averages, centre frequencies at 500 Hz, 1000 Hz and 1500 Hz. ·····, $\gamma_0 = 1$.

[13]. Figure 14 shows this power ratio for frequency average powers, the ratio being close to unity for all geometries and centre frequencies over a range of μ_0 . It may be inferred from this that SEA is applicable to such 2-plate systems so long as the appropriate coupling

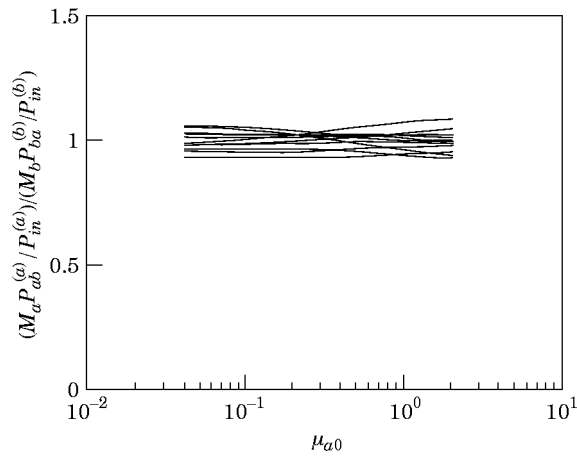


Figure 14. “Reciprocity”: power ratios as a function of base reflectance of smaller plate, 9 two-plate systems.

loss factor is used, this differing from the traditional, asymptotic expression (equation (8)) and being dependent on subsystem geometry when the coupling is strong.

5. CONCLUDING REMARKS

This paper concerned the SEA of systems comprising two coupled plates. Numerical estimates of frequency average powers and coupling loss factors were found from FE models of the systems. These were compared with theoretical predictions found from traditional, asymptotic SEA and an analytical solution applicable to coupled, rectangular plates. While there are of course dangers in drawing conclusions from a limited number of numerical examples of the behaviour of individual systems, the results presented are typical and support the following conclusions.

There is a qualitative difference between the behaviours at low and high levels of damping, more specifically, for the cases of strong and weak coupling. For high enough damping (i.e., weak coupling), the detailed subsystem geometry is unimportant and the traditional, asymptotic theory gives accurate predictions. However, for lighter damping, so that the coupling is strong, the coupling power depends significantly on subsystem irregularity. The asymptotic theory overestimates both the coupling power and the coupling loss factor, particularly for the case of rectangular plates. These effects are of course in accordance with the observation that SEA “works best” when applied to irregular systems.

One implication is that if the coupling is strong, more information about each subsystem is required to give accurate response predictions than is normally used in SEA models—e.g., not only the area but also the shape of each plate subsystem is important in determining the ensemble or frequency average response. Energy flow methods are currently deficient in this regard.

The behaviour observed was interpreted in terms of localisation of the global mode shapes of the system and in terms of coherence of waves incident upon the coupling: increasing irregularity tends to “spread out” the mode shapes across the system and to scatter waves into different directions of propagation so that coherence effects are reduced.

The coupling parameter γ_0 (i.e., the maximum value of γ given by equation (10)) can be used to give an estimate of the strength of coupling. This parameter indicates the relative strengths of transmission through the coupling and of damping within the subsystems. To a good approximation, for these edge coupled plates

$$\gamma_0^2 = T^2 / \mu_{a0} \mu_{b0}, \quad (20)$$

where the base reflectances indicate the effects of damping and are given by

$$\mu_0 = \eta k A / 2d \quad (21)$$

For rectangular plates μ_0 rather than modal overlap M , is the appropriate parameter with which to describe the effects of damping. The parameter γ_0 gives a conservative estimate of coupling strength for irregularly shaped subsystems.

Finally it is worth noting that in most structural applications the levels of damping, the magnitudes of transmission coefficients and the frequency ranges involved are such that the coupling is strong. Moreover, plates tend to be rectangular rather than highly irregular, so that the effects described here are likely to be quite widespread.

REFERENCES

1. R. H. LYON 1975 *Statistical Energy Analysis of Vibrating Systems*. Cambridge, MA: MIT Press.
2. L. CREMER, M. HECKL and E. E. UNGAR 1988 *Structure-Borne Sound*. Berlin: Springer-Verlag; second edition.
3. E. C. N. WESTER and B. R. MACE 1996 *Journal of Sound and Vibration* **193**, 793–822. Statistical energy analysis of two, edge-coupled, rectangular plates—ensemble averages.
4. B. R. MACE and P. J. SHORTER Energy flow models from finite element analysis submitted to the *Journal of Sound and Vibration*.
5. C. R. FREDÖ 1995 *Journal of Sound and Vibration* **185**, 867–890. A SEA-like approach for the derivation of energy flow coefficients with a finite element model.
6. C. BOISSON, J. L. GUYADER, P. MILLOT and C. LESUEUR 1982 *Journal of Sound and Vibration* **81**, 93–105. Energy transmission in finite coupled plates, Part 2: application to an L-shaped structure.
7. E. K. DIMITRIADIS and A. D. PIERCE 1988 *Journal of Sound and Vibration* **123**, 397–412. Analytical solution for the power exchange between strongly coupled plates under random excitation: a test of statistical energy analysis concepts.
8. F. J. FAHY and A. D. MOHAMMED 1992 *Journal of Sound and Vibration* **158**, 45–67. A study of uncertainty in applications of SEA to coupled beam and plate systems, part 1: computational experiments.
9. C. SIMMONS 1991 *Journal of Sound and Vibration* **144**, 215–227. Structure-borne sound transmission through plate junctions and estimates of SEA coupling loss factors using the FE method.
10. B. R. MACE 1997 *Journal of Sound and Vibration* **199**, 369–380. Wave coherence, coupling power and statistical energy analysis.
11. B. R. MACE 1993 *Journal of Sound and Vibration* **166**, 429–461. The statistical energy analysis of two continuous one-dimensional subsystems.
12. B. R. MACE 1996 *Journal of Sound and Vibration* **189**, 443–476. Finite frequency band averaging effects in the statistical energy analysis of two continuous one-dimensional subsystems.
13. B. R. MACE 1994 *Journal of Sound and Vibration* **178**, 95–112. On the statistical energy analysis hypothesis of coupling power proportionality and some implications of its failure.
14. A. D. MOHAMMED 1990 *Ph.D. Thesis, University of Southampton*. A study of uncertainty in applications of statistical energy analysis.
15. B. R. MACE and P. J. SHORTER 1997 *IUTAM Symposium on SEA, Southampton*. Irregularity, damping and coupling strength in SEA.

APPENDIX: LIST OF SYMBOLS

A	area
B	bending stiffness
c_g	group velocity
d	length of coupled edge
D	energy density
E	energy
F	force
k	wavenumber
l	plate length, rectangular plate
m	mass per unit area
M	modal overlap
n	asymptotic modal density
P_{ab}	coupling power from subsystem a to subsystem b
P_{diss}	dissipated power
P_m	input power
P_{inc}	incident power
T	transmission coefficient, kinetic energy
V	potential energy
α	modal receptance, equation (13)
γ, δ	coupling parameters, equation (10)
γ_0	$\max(\gamma)$

Δ	half-power bandwidth
η	damping, coupling loss factor
κ	ratio of trace wavenumber to wavenumber
λ	modal kinetic energy localisation factor
μ	reflectance
μ_0	base reflectance, equation (10)
ϕ	mode shape
ψ	modal kinetic energy distribution factor, equation (32)
ω	frequency
Ω	averaging bandwidth
$\langle \cdot \rangle$	ensemble average
$\bar{\cdot}$	frequency average
<i>Subscripts</i>	
a, b	plate
∞	asymptotic, infinite value